

2011

## The design of a computer system to determine the causes of edema using magnetic resonance spectroscopy

Carl Allen Fink

*Louisiana State University and Agricultural and Mechanical College*

Follow this and additional works at: [https://repository.lsu.edu/gradschool\\_theses](https://repository.lsu.edu/gradschool_theses)



Part of the [Computer Sciences Commons](#)

---

### Recommended Citation

Fink, Carl Allen, "The design of a computer system to determine the causes of edema using magnetic resonance spectroscopy" (2011). *LSU Master's Theses*. 3919.

[https://repository.lsu.edu/gradschool\\_theses/3919](https://repository.lsu.edu/gradschool_theses/3919)

This Thesis is brought to you for free and open access by the Graduate School at LSU Scholarly Repository. It has been accepted for inclusion in LSU Master's Theses by an authorized graduate school editor of LSU Scholarly Repository. For more information, please contact [gradetd@lsu.edu](mailto:gradetd@lsu.edu).

THE DESIGN OF A COMPUTER SYSTEM TO DETERMINE THE CAUSES OF  
EDEMA USING MAGNETIC RESONANCE SPECTROSCOPY

A Thesis

Submitted to the Graduate Faculty of the  
Louisiana State University and  
Agricultural and Mechanical College  
in partial fulfillment of the  
requirements for the degree of  
Master of Science in Systems Science

in

The Department of Computer Science

by

Carl Fink

B.S., Loyola University New Orleans, 2003

May 2011

# Table of Contents

List of Figures . . . . .	iii
Abstract . . . . .	iv
<b>1 Introduction . . . . .</b>	<b>1</b>
<b>2 Background . . . . .</b>	<b>2</b>
2.1 Magnetic Resonance Imaging . . . . .	2
2.2 Magnetic Resonance Spectroscopy . . . . .	2
2.2.1 Frequency Domain . . . . .	2
2.2.2 Chemical Shift . . . . .	4
2.2.3 Spin-Spin Scalar Coupling . . . . .	5
2.2.4 Quantification of Chemical Shifts . . . . .	6
2.3 Proton Spectroscopy MRI . . . . .	7
2.4 Two-dimensional Correlated Spectroscopy . . . . .	8
<b>3 Previous Work . . . . .</b>	<b>10</b>
<b>4 Approach . . . . .</b>	<b>12</b>
4.1 Neural Networks . . . . .	12
4.2 Methodology . . . . .	12
<b>5 Conclusions . . . . .</b>	<b>14</b>
References . . . . .	15
Vita . . . . .	18

## List of Figures

1	$T_1$ -weighted spin echo image of a 10% ethanol solution. . . . .	3
2	The free induction decay (FID) process of 10% ethanol solution shown in Figure 1. . . . .	3
3	The Fourier transform of the FID shown in Figure 2. . . . .	4
4	2-D COSY contour plot of lactic acid demonstrating a two-dimensional plot with symmetric cross peaks that represent scalar-coupled resonances of lactic acid. . . . .	9

# Abstract

Diabetes is a growing problem in the U.S.A., closely linked to the current obesity epidemic. Two common complications of diabetes, osteomyelitis of the foot, and Charcot's joint, are impossible to differentiate via traditional Magnetic Resonance Imaging. The background of Magnetic Resonance Spectroscopy, which transforms the time-domain MRI signal into the frequency domain spectrum, is explored, and its use to aid in this differentiation is proposed. Artificial Neural Networks can be employed to evaluate the MRS data and to automate the process.

# 1 Introduction

Diabetes is a growing problem in the U.S.A. It is closely linked to the current obesity epidemic. The diabetic ulcer is an exceedingly common complication of advanced stages of this disease. It is commonly associated with poor circulation, which, in combination with other complications of diabetes, predisposes a patient to osteomyelitis of the foot. Another disease commonly associated with diabetes is Charcot's joint due to diabetic neuropathy. These distinct processes have multiple overlapping Magnetic Resonance Imaging findings, which often make differentiation of the two impossible via traditional MRI. Another study, such as a nuclear scan, is typically required to differentiate the two processes.

In this research, the use of MR spectroscopy is proposed to differentiate the causes of edema by detecting differences in metabolite levels within the bones of the foot, arthritides and osteomyelitis. Because of their value in classification problems, this research will employ neural networks to expedite this important detection.

## 2 Background

### 2.1 Magnetic Resonance Imaging

Magnetic Resonance Imaging is a medical imaging tool used in radiology to visualize internal structures. It uses a powerful magnetic field to align the magnetization of some atoms in the body, then applies radio frequency fields to systematically alter the alignment of this magnetization. This induces the atoms' nuclei to produce a rotating magnetic field, which is recorded by the scanner, and then assembled to produce an image of the scanned area.

### 2.2 Magnetic Resonance Spectroscopy

Magnetic Resonance Spectroscopy (MRS) relies on the same basic techniques used in MRI. The principle difference is the manner in which the acquired data is presented [26].

#### 2.2.1 Frequency Domain

MRI uses a signal obtained in the time domain to generate an image. MRS uses the Fourier transform of the MR signal, which is in the time domain to generate a frequency domain spectrum of the components that comprise the image.

Figure 1 shows a  $T_1$ -weighted spin echo image of a 10% ethanol solution. Figure 2 shows the free induction decay process of the MR signal arising from the protons associated with water and ethanol versus time; this is used to generate the image in Figure 1. The time decay process is characterized by

$$I = e^{-kt/T}$$

where  $I$  is the intensity of the signal at time  $t$ ,  $k$  is a constant, and  $T$  is the relaxation time of the nuclei being excited.

It is difficult to determine which part of the image in Figure 1 is composed of protons from ethanol. However, a Fourier transformation of the time-domain signal results in a frequency distribution of the proton components that make up the time domain signal (Figure 3). This frequency spectrum reveals which part of the time domain signal arises from the protons of the methyl ( $\text{CH}_3$ ) and which part is from the methylene ( $\text{CH}_2$ ) groups of ethanol.

Why, then, do the protons of water appear at different regions of the frequency domain than those of the methyl and methylene groups of ethanol? Nuclear magnetic resonance (NMR) is based on the principle that nuclei have an associated spin property, which causes them to behave like small magnets [14, 26]. In the presence of a magnetic field, the nuclei interact with the magnetic field, distributing themselves to different levels.

In the case of protons, which have a "spin quantum number" of  $\frac{1}{2}$ , the nuclei distribute themselves into two distinct states, corresponding to their spin in either the direction of or the direction opposite the applied magnetic field. The separation between levels is proportional

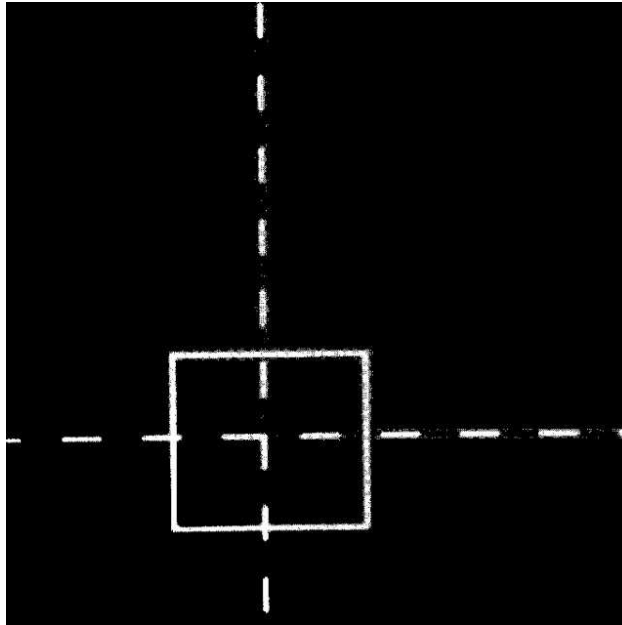


Figure 1:  $T_1$ -weighted spin echo image of a 10% ethanol solution.

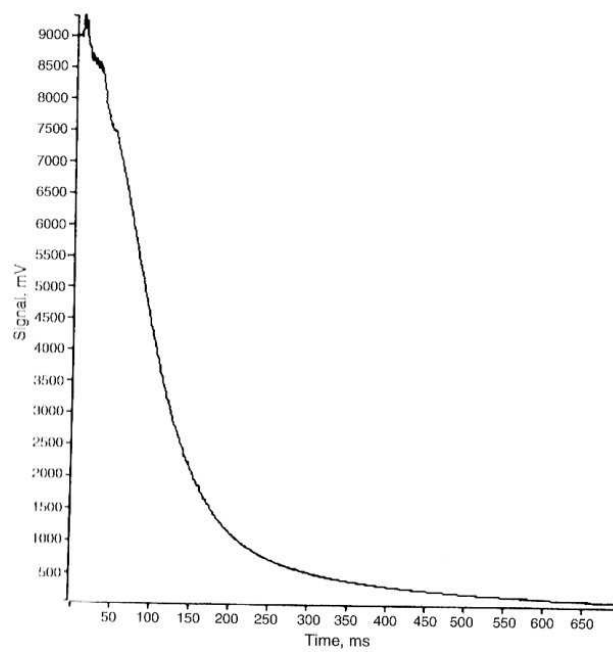


Figure 2: The free induction decay (FID) process of 10% ethanol solution shown in Figure 1.



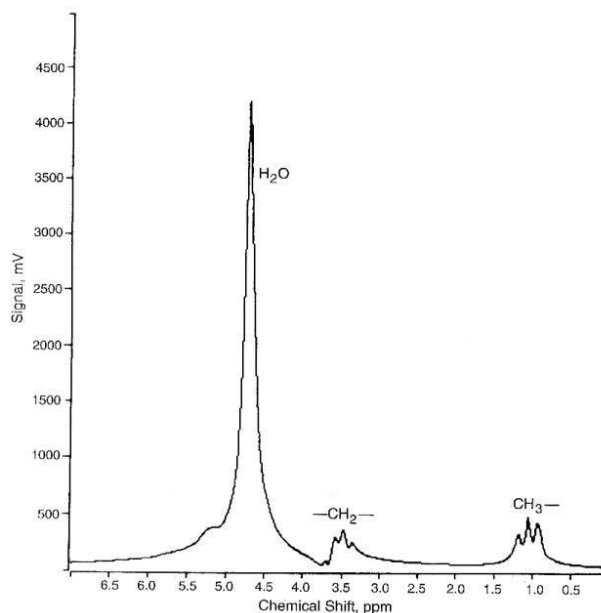


Figure 3: The Fourier transform of the FID shown in Figure 2.

to the strength of the applied magnetic field; as the magnetic field strength increases, so does the intensity of the signal. This is partly the result of the increase in energy separation between the two states, and partly because of the increase in the number of nuclei in a lower-energy state that can be excited to a higher-energy state [14].

If energy is applied in the form of a radiofrequency wave that exactly matches the energy separation between the two energy states, then a “resonance” occurs. Nuclei in the lower-energy state absorb this resonance energy and are promoted to the higher-energy state. This phenomenon is described by the Larmor frequency equation,

$$\Delta E = \kappa\omega_0 = \kappa\gamma B_0 \quad (1)$$

where  $\omega_0$  is the Larmor precessional frequency (Hertz),  $\kappa$  is the Planck constant divided by  $2\pi$ ,  $\gamma$  is the gyromagnetic ratio for each nucleus (megahertz per Tesla), and  $B_0$  is the applied magnetic field (Elsa).

### 2.2.2 Chemical Shift

The Larmor frequency equation (1) states that the resonance frequency of a magnetic nuclei (the radiofrequency necessary to excite a given nuclei) is directly proportional to the magnetic field environment it experiences. Different atoms resonate at different Larmor radiofrequencies because their nuclei have different magnetic spin properties. This is the basis for the NMR phenomenon and allows the identification of magnetic nuclei with different atomic numbers. However, even for another magnetic nuclei or atom with the same atomic number, chemical compounds containing this nuclei may have slightly different Larmor res-

onance frequencies. This results from the electrons that surround the nuclei, forming the electron cloud.

Electrons are negatively charged, and, like protons and neutrons, also have spin properties. Thus, when placed in a magnetic field, electrons will produce a small magnetic field  $B'$  around the nuclei. These local magnetic fields generated by the surrounding electrons can add to or subtract from the applied field  $B_0$ . Consequently, the nuclei experiences a slightly different magnetic field  $B_{\text{eff}}$ , which is equal to  $B_0 - B$ . Because of this small change in the local magnetic field, the nucleus will resonate with a slightly shifted Larmor frequency, since the frequency is the product of the gyromagnetic ratio and the local magnetic field strength experienced by the nucleus. This phenomenon is called the *chemical shift* and is the basis for MRS.

This explains why the protons of ethanol (Figure 3) have different Larmor frequencies. The molecular structure of ethanol is such that the hydrogen nuclei (protons) are found in three different atomic groups in the molecule, and experiences the effects of three different electron cloud distributions. The local magnetic field of these three positions differ slightly, and each of these hydrogen nuclei resonates at a frequency characteristic of its position in the molecule. Consequently, the proton spectrum of ethanol (Figure 3) depicts different resonate frequencies: one for the  $\text{CH}_3$  protons; another for the  $\text{CH}_2$  protons.

### 2.2.3 Spin-Spin Scalar Coupling

The protons in the methyl group and methylene in ethanol are composed of three and four resonate frequencies, respectively. This is the result of the quantum mechanical phenomenon of *spin-spin coupling* or *splitting*. The observations of these frequency-splitting patterns are explained by the magnetic field of one proton influenced by the arrangement of the spin orientations of adjacent groups. Nuclei with a net spin quantum number of  $\frac{1}{2}$  in the direction of the applied magnetic field or in a direction  $180^\circ$  opposed to it are affected. For the three protons of the methyl group of ethanol, there are three possible spin orientations for the protons in the adjacent methylene group. These spin orientations correspond to different energy levels and using the Larmor frequency (1) leads to three different magnetic fields or energy levels. Nuclei in adjacent groups interact with these energy levels. The interaction affects the methyl protons by splitting their single resonance frequency into three resonance frequencies, which correspond to the three energy levels or orientations of the adjacent methylene group, with which they can interact once they have absorbed energy. This produces three resonance peaks observed in the frequency spectrum for the methyl protons of ethanol. Peak area ratios of 1 : 2 : 1 are caused by the three possible spin orientation interactions for the methylene protons. The middle resonance is double the intensity of the two side resonances, because there are twice as many spin combinations with the same total energy that produces this state. Similarly, the methylene resonance is split

into four resonant frequency peaks by the four spin arrangements possible for the protons on the neighboring methyl group. The relative peak area intensities of the four methylene resonances are in the ratio of 1 : 3 : 3 : 1 because of the spin orientation arrangement of the methyl protons.

In addition, the methyl and methylene proton resonances are 180° out of phase with respect to each other. This is the result of the pulse sequence used to acquire the spectra. Out-of-phase resonances in homonuclear spin-coupled multiplets are a characteristic feature when spin echo pulse sequences are used to obtain the spectra and depend on this tau-value. This out-of-phase effect is caused by changes in the spin states of homonuclear spin-coupled systems when a 180° pulse is used.

Presently, the clinical significance of the spin-spin coupling phenomenon is limited to the identification of lactate in several pathologic processes [30]. However, when clinical facilities with higher field magnets begin to perform more in vivo MRS on patients, spin-spin coupling will become more relevant in the identification of important metabolites, because the higher resolution of these systems allows separation of overlapping resonances [16]. In addition, preliminary in vivo human brain studies using two-dimensional correlated spectroscopy techniques at 1.5 T have been performed [32]. This technique examines nuclei that are spin coupled and increases the ability to identify other important proton metabolites.

#### 2.2.4 Quantification of Chemical Shifts

Chemical shifts are usually measured relative to the peak position of an arbitrary reference compound or the center Larmor carrier frequency of the spectrometer for nuclei at the field strength being used. In the case of in vivo brain proton MRS, *N*-acetylaspartate (NAA) is normally chosen as the internal reference compound and is set at 2 ppm in the spectrum. The frequency position of this resonance is separated by a factor of 2ppm from the center radiofrequency of the spectrometer.

In practice, when displaying spectra, the frequencies are not expressed in absolute units, e.g. Hertz. If the chemical shift is reported in Hertz, then the chemical shift would depend on the magnetic field. It is preferable to refer to the chemical shift as a relative value  $\delta$  and to define it as the frequency separation between the resonance peak and the reference Larmor frequency for the nuclei under investigation divided by the operating spectrometer frequency or the magnetic field  $B_0$ :

$$\delta = (B_i - B_{ref})/B_0 \times 10^{-6} = (\omega_i - \omega_r)/\omega_0 \times 10^{-6} \quad (2)$$

where  $B_i$  and  $\omega_i$  are the radiofrequency and magnetic field at which resonance occurs for the nuclei being described, and  $B_0$  and  $\omega_0$  are the magnetic field and the center Larmor radiofrequency of the nuclei under investigation (for protons at 1.5 T, this value is 63.86

mHz; for phosphorus at 1.5 T, it is 25.85 mHz).  $\delta$  is dimensionless and is measured in parts per million. The ppm unit is used because the resonance frequency is in megahertz ( $10^6$  Hz), but the difference between the reference peak and the compound peak is only a few hertz. Therefore, this ratio is on the order of  $10^{-6}$ , or parts per million. Multiplication by  $10^6$  produces a more convenient  $\delta$  number (between 0 and 10 ppm for protons). The significance of  $\delta$  is that chemical shift positions of the nuclei with the same atomic number measured in ppm are independent of the field strength used.

## 2.3 Proton Spectroscopy MRI

Protons are widely used for MRS because of their high natural abundance in organic substances and high nuclear magnetic sensitivity, especially compared to phosphorus [6]. In addition, diagnostically resolvable hydrogen MR spectra may be obtained with existing MR units ( $\geq 1.5$  T) and standard head coils [6]. Typically, investigators evaluate for changes in levels of *N*-acetylaspartate (NAA), choline (Cho), and creatine (Cr). Early studies looking at brain tumors and cerebral infarctions have validated the use of  $^1\text{H}$  MRS in the evaluation of neurological abnormalities.

Recent and preliminary reports for single-volume  $^1\text{H}$  MRS show promising but variable results in the evaluation of mesial temporal lobe seizures [7, 8, 10, 12]. Most of these studies demonstrate a decrease in the NAA and NAA:Cr ratio or in the NAA and NAA:(Cho+Cr) ratio [7, 10, 12], while others have reported only low concentration of NAA without the changes in the levels of Cr and Cho [11, 13]. Increases in Cr and Cho have, however, also been reported [8, 12]. Common to all  $^1\text{H}$  MRS studies is the decrease in NAA in the affected temporal lobes of intractable epilepsy patients compared to normal controls. Reduction in NAA may be interpreted as neuronal loss or damage, a frequent *in vitro*  $^1\text{H}$  MRS finding when examining seizure foci [17]. This finding is supported by pathologic studies that have shown that there is extensive neuronal loss and reactive astrogliosis in the affected HC and in the adjacent temporal lobe. The magnitude of the decrease in NAA is too great to be explained by loss or damage to only the mesial temporal neurons and likely reflects the widespread damage in the adjacent regions of the temporal lobe [17]. This may explain the abnormalities detected on MRS studies in which the volume of interest (VOI) encompassed far more than just the HC. Therefore, despite the integration of normal-appearing tissues into a VOI, partial volume artifacts may not be significant in patients with hippocampal seizures. It is likely that the changes in the aforementioned ratios merely reflect a decrease in NAA and are unrelated to Cr and Cho. Some researchers have chosen not to use Cr or Cho ratios in spectral analysis because, when the metabolic values are expressed as ratios, it is often impossible to determine what the findings reflect [28].

## 2.4 Two-dimensional Correlated Spectroscopy

One-dimensional proton magnetic resonance spectroscopy (NMRS) is a highly sensitive technique that permits the detection of numerous metabolites in living tissues under normal and pathologic conditions. However, the chemical shift range of proton spectra is relatively narrow, which leads to overlapping resonances. This overlap makes the assignment of resonances to specific protons difficult. In clinical applications of NMRS, the problem of overlapping resonances may be more severe due to broadening of the spectral peaks and the complexity of spectra of cells and tissues [5].

Two-dimensional NMR methods can be employed to separate the composite 1-D spectral MRS resonances into their component peaks by the generation of cross-peaks in a second dimension. These cross-peaks provide information necessary for the identification of additional metabolites that are not visible in the one-dimensional spectrum. Thus, 2-D NMR has the potential for providing useful information in the clinical environment beyond that currently available through 1-D proton NMR.

The basic 2-D NMR sequence, scalar correlated spectroscopy (2-D COSY), provides a technique for identifying metabolites by identifying protons that are spin-coupled [15, 25]. Spin-coupling results from the different environments generated by interactions between the hydrogen atoms within a molecule. The spinning of a proton generates a magnetic moment along the axis of the spin, caused by the spinning charge. This results in a local magnetic field around each proton. The interactions between the local magnetic fields of adjacent protons alter the effective field strength that the proton “feels.” The effective field strength of a proton may be slightly increased or decreased, depending on whether the neighboring proton is aligned with or against the applied field at any given instant. This change in effective field strength changes the frequency at which the proton absorbs energy, resulting in spin-spin splitting, since the spin of one nucleus causes a change in the energy levels of a nearby nucleus.

The result of the 2-D COSY sequence is a two-dimensional plot that contains a series of cross-peaks. Figure 4 shows a 2-D COSY contour plot of lactic acid. These off-diagonal cross-peaks show which resonances on the diagonal are scalar-coupled, allowing the resonances to be assigned to specific molecules or compounds [9, 19, 21].

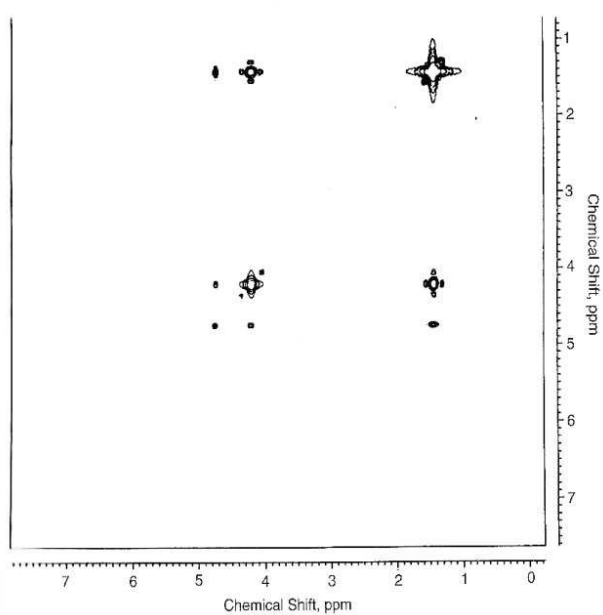


Figure 4: 2-D COSY contour plot of lactic acid demonstrating a two-dimensional plot with symmetric cross peaks that represent scalar-coupled resonances of lactic acid.

### 3 Previous Work

2-D NMR has been used to evaluate cells and tissue to identify resonances that were not resolvable using 1-D proton NMR. For example, Mountford et al. [21] used detailed information on the lipid resonances obtained through 2-D NMR techniques to detect changes in cellular chemistry that occur during the transformation of normal cells to neoplastic cells and in the progression of malignant disease. The additional resonances allowed them to discriminate between control, immunostimulated, and tumor-bearing lymph nodes from rats. Specifically, the tumor-bearing nodes had more intense cross-peaks of lactate, choline, fucose, and amino acids than did the normal or immunostimulated node.

In a study of human cells, Lean et al. [15] demonstrated the use of 2-D proton MRS for distinguishing between a highly tumorigenic human malignant colorectal cell line and a lowly tumorigenic cell line of similar origin. An altered lipid profile, higher choline metabolite content, and more complex cell surface fucosylation allowed the discrimination of the highly tumorigenic cells from the less tumorigenic cells. Mackinnon et al. [18] further developed this distinction, providing a correlation between an increase in the complexity of cell surface fucosylation and cellular differentiation in a well-defined series of adenoma and carcinomal colorectal cell lines and tissues.

Lean et al. [16] reported the ability to assess the cellular dedifferentiation using MRS profiles of colorectal tissues and to discriminate between tumor and normal colorectal mucosa. They also reported that the spectral patterns identified two categories within the normal mucosa, one of which had some of the MR characteristics of malignancy, specifically the appearance of cross-peaks from bound fucose. They suggest that these findings may indicate a mechanism for characterizing abnormal nonmalignant colorectal tissues with proton MRS. They further suggest that these findings may contribute to the understanding of the process of transformation of tissues from normal to malignant state.

High-resolution proton NMR studies of intact cancer cells also has provided information on differences between cells with the capacity to metastasize and those that produce locally invasive tumors. Mountford et al. [20] used high-resolution NMR to assess the metastatic potential of primary tumors. They demonstrated that the component resonances in the lipid methylene region at 1.2 ppm could provide information on the biologic status of intact cancer cells. They concluded that the ability of cells to metastasize might be attributed in part to cell membrane characteristics, which are determined in part by the modulating effects of the plasma membrane lipids. NMR resonances that characterized the metastatic cells were associated with an increased ratio of cholesterol to phospholipid and an increased amount of plasma membrane-bound cholesterol ester. This was supported by the work of Sivaraja et al. [27] in a study of smooth muscle tumors (leiomyosarcoma) and benign tissues (leiomyoma) that evaluated the relationship between metastatic potential and differences in triglycerides and carbohydrates information from the NMR spectra. May et al. [19] and

Williams et al. [33] used high-resolution 2-D NMR to further analyze cell suspensions to identify these resonances as arising predominantly from triglyceride in the plasma membranes and from soluble nonlipid components. This increase in the relative amounts of neutral lipid-triglyceride in the membrane may result in changes in the permeability properties of the membranes.

Mukherji et al. [23] evaluated the use of 2-D COSY in the analysis of tissue specimens of human squamous cell carcinomas of the extracranial head and neck. The goal was to ascertain which cross-peaks in the 2-D COSY spectra could be used to discriminate between tumor and normal tissues. Data were analyzed for the presence or absence of the cross-peaks for choline, phosphocholine, glycerophosphocholine, alanine, glycine, glutamine, histidine, leucine, isoleucine, valine, inositol, taurine, lactate, triglycerides A-G, fucose-threonine, and lysine-polyamine. Chi-square analysis indicated that the cross-peaks for alanine, glutamine, histidine, isoleucine, valine, and lysine-polyamine were more likely to be detected in tumor samples than in normal tissues. The spectra generated from tumor tissue were considerably more complex than those from normal tissue and contained lipid peaks that were smaller and less elliptical than those in normal tissue spectra.

2-D NMR has also been used *in vivo* to resolve resonances that overlap in the 1-D spectra. This was demonstrated by Sotak et al. [29], who employed 2-D NMR to distinguish between lipid and lactate in a localized volume, using a surface coil over Radiation Induced Fibrosarcoma-1 (RIF-1) tumors implanted subcutaneously on the back of a mouse. Peres et al. [24] measured the total glucose pool in rat brains by 2-D NMR using a surface coil. The surface coil was placed directly on the skull of a rat. They reported a linear relationship between cross-peak volume and concentration but could not measure absolute concentrations because of the lack of an internal reference. The 2-D spectra also allowed resolution of the inositol and taurine peaks which were not visible in the 1-D spectra.



## 4 Approach

### 4.1 Neural Networks

The human brain is an example of a biological neural network. It contains many billions of cells known as nerve cells or *neurons*. These cells are organized into a complex intercommunicating network. Each neuron is physically connected to tens of thousands of others. Using these connections, neurons pass electrical signals to one another. These connections are not merely on or off; they have varying strength, allowing the influence of a given neuron on its neighbors to be very strong, very weak, or anywhere in between. Furthermore, many aspects of brain function (particularly the learning process) are closely associated with the adjustment of these connection strengths. Brain activity, then, is represented by particular patterns of firing activity among this network of neurons. This simultaneous cooperation among a myriad of simple processing units is the basis of the enormous sophistication and computational power of the brain.

An artificial neural network (ANN) is a computational model whose architecture is modeled after the brain. It consists of many simple processing units which are connected together in a complex communication network [1]. In most cases an ANN is an adaptive system whose structure changes based on information flowing through the network. This allows ANNs to be “trained” to solve certain types of problems. In this way, ANNs have shown themselves to be quite effective at classification problems, including pattern and sequence recognition and novelty detection.

The most basic ANN has three layers, including a layer of input neurons and a layer of output neurons. More complex systems are possible, with more layers, and various “weights” assigned to each processing unit, which manipulates the data in the calculations.

The ability of an ANN to *learn* is what makes them especially powerful. Given a specific problem, and a class of functions  $F$ , an ANN can “learn” by using a set of observations to find the function  $f^* \in F$ , an *optimal* solution to the problem.

This optimal solution is can be defined by specifying a cost function  $C : F \rightarrow \mathbb{R}$  such that, for the optimal solution  $f^*$ ,  $C(f^*) \leq C(f) \forall f \in F$ . That is to say, no alternate solution has a cost less than that of the optimal solution.

### 4.2 Methodology

It is with this in mind that we intend to differentiate causes of edema within the bones of the foot. One of the most common causes of such edema is arthritis. Also common is osteomyelitis, an infection of the bone or bone marrow.

We shall use artificial neural networks to test the hypothesis that there is a significant difference in pH between infected bone edema and non-infected edema, as seen in Charcot’s

joint, which can be detected via MR Spectroscopy. This is a novel approach to solving the diagnosis problem, as it is based on a fundamentally different method of differentiating the causes of edema than those traditionally used.

For our ANN, the function  $f(x)$  by which we will evaluate metabolite levels is defined as a composition of other functions  $g_i(x)$ . This composition is a *nonlinear weighted sum*

$$f(x) = K\left(\sum_i w_i g_i(x)\right)$$

where  $K$  is a function measuring the metabolite level of the input spectroscopy data.

In order to make this determination, we require MR Spectroscopic data on a number of patients, where the determination of whether each patient's data represents infected or non-infected edema has already been made by a pathologist. One problem that often plagues studies of this sort is that of insufficient data. Ideally, one would like to have a large statistical sample to experiment with. Often, a large amount of data is difficult or impossible to come by; one simply has to do the best he can with the data available.

To circumvent this problem, we can use one-half of this data set to “train” our ANN to make the determination between infected bone edema and non-infected edema. This will allow us to then use the trained ANN on the remaining data. We measure the metabolite level of the input spectroscopy data, using that information as the input into our evaluation function, so that the value given by  $f$  ultimately predicts the cause of edema in a given case, which we expect will match the determination already made by the pathologist. By comparing it to this previously-made determination, we can gauge the accuracy of this trained ANN, illustrating the rate of success with which it can be used to differentiate the two different causes of edema within the bones of the foot.

Depending on this rate of success, our ANN's training can be further refined by using the second half of the data set as a second training set. The results of this additional training can be evaluated by using it to make the edema cause determination, and again comparing the results to those determined by the traditional method. The data can then be further re-arranged, using a different subset each time for training, making predictions about the remaining data based on that training. It is our assertion that this design will prove successful, demonstrating that a sufficiently-trained ANN can indeed be used to differentiate the causes of edema within the bones of the foot. If this is the case, it should prove a valuable diagnostic tool, as additional tests (such as a nuclear scan) will not be necessary in making this determination.

## 5 Conclusions

There are over 5,000 hospitals operating in the United States [3], supporting approximately 3,000 radiology practices [31]. With approximately 1 in 62 people suffering from edema [2], there are myriad opportunities to improve the diagnosis of its causes. By developing a robust diagnostic tool, this evaluation could be made quicker and more efficient, and thanks to the refinement of ANNs, with great accuracy.

With thousands of radiology departments performing numerous such diagnoses, this approach has the potential to produce great savings in time and resources, and to contribute to the health and well-being of patients sufferent from edema.

## References

- [1] Herv Abdi. "A Neural Network Primer." *Journal of Biological Systems*, 1994: 247-283.
- [2] Australian Bureau of Statistics 2001 National Health Survey. "Australia's Health 2004." Australian Institute of Health and Welfare. 2004.
- [3] American Hospital Association. "Fast Facts on U.S. Hospitals." <http://www.aha.org/> 2010.
- [4] Yaneer Bar-Yam. *Dynamics of Complex Systems*, 2003.
- [5] K.L. Behar, T. Ogino. "Assignment of Resonances in the  $^1\text{H}$  Spectrum of Rat Brain by Two-dimensional Shift Correlated and J-resolved NMR Spectroscopy." *Magn Reson Med*, 1991.
- [6] M. Castillo, L. Kwock, S.K. Mukherji. "Clinical Applications of Proton MR Spectroscopy." *AJNR*, 1996.
- [7] F. Cendes, F. Andermann, M.C. Preul, et al. "Lateralization of Temporal Lobe Epilepsy Based on Regional Metabolic Abnormalities in Proton Magnetic Resonance Spectroscopic Images." *Ann Neurol*, 1994.
- [8] A. Connelly, G.D. Jackson, J.S. Duncan, et al. "Magnetic Resonance Spectroscopy in Temporal Lobe Epilepsy." *Neurology*, 1994.
- [9] K.J. Cross, K.T. Holmes, C.E. Mountford. "Assignment of Acyl Chain Resonances from Membranes of Mammalian Cells by Two-dimensional NMR Methods." *Biochemistry*, 1984.
- [10] J.H. Cross, A. Connelly, G.D. Jackson, et al. "Proton Magnetic Resonance Imaging in Children with Temporal Lobe Epilepsy." *Ann Neurol*, 1996.
- [11] C.M. Epstein, D. Boor, J.C. Hoffman, et al. "Evaluation of  $^1\text{H}$  Magnetic Resonance Spectroscopic Imaging as a Diagnostic Tool for the Lateralization of Epileptogenic Seizure Foci." *Br J Radiol*, 1996.
- [12] D.G. Gadian, J.S. Duncan, F.J. Kirkham, et al. " $^1\text{H}$  Magnetic Resonance Spectroscopy in the Investigation of Intractable Epilepsy." *Acta Neurol Scand*, 1994.
- [13] J.W. Hugg, K.D. Laxer, G.B. Matson, et al. "Neuron Loss Localized Human Temporal Lobe Epilepsy by in Vivo Proton Magnetic Resonance Spectroscopic Imaging." *Ann Neurol*, 1993.
- [14] J.A. Koutcher, C.T. Burt. "Principles of Nuclear Magnetic Resonance." *J Nucl Med*, 1984: 101-111.
- [15] C.L. Lean, W.B. Mackinnon, E.J. Delikatny, et al. "Cell-Surface Fucosylation and Magnetic Resonance Spectroscopy Characterization of Human Malignant Colorectal Cells." *Biochemistry*, 1992.
- [16] C.L. Lean, R.C. Newland, D.A. Ende, et al. "Assessment of Human Colorectal Biopsies by  $^1\text{H}$  MRS: Correlation with Histopathology." *Magn Reson Med*, 1993.

- [17] J.H. Margerison, J.A.N. Corsellis. "Epilepsy and the Temporal Lobes: A Clinical, Electroencephalographic and Neuropathological Study of the Brain in Epilepsy with Particular Reference to the Temporal Lobes." *Brain*, 1966.
- [18] W.B. Mackinnon, G.L. May, C.E. Mountford. "Esterified Cholesterol and Triglyceride Are Present in Plasma Membranes of Chinese Hamster Ovary Cells." *Eur J Biochem*, 1992.
- [19] G.L. May, L.C. Wright, K.T. Holmes, et al. "Assignment of Methylene Proton Resonances in NMR Spectra of Embryonic and Transformed Cells to Plasma Membrane Triglycerides. *J Biol Chem*, 1986.
- [20] C.E. Mountford, L.C. Wright, K.T. Holmes, et al. "High-resolution proton nuclear magnetic resonance analysis of metastatic cancer cells." *Biochem Biophys Methods*, 1984.
- [21] C.E. Mountford, C.L. Lean, R. Hancock, et al. "Magnetic Resonance Spectroscopy Detects Cancer in Draining Lymph Nodes." *Invasion Metastasis*, 1993.
- [22] Suresh K. Mukherji, M.D.. *Clinical Applications of MR Spectroscopy*. Wiley-Liss, Inc., 1998.
- [23] Suresh K. Mukherji, S. Schiro, M. Castillo, et al. "MR Proton Spectroscopy of Squamous Cell Carcinoma of Extracranial Head and Neck: In Vitro and In Vivo Studies" *AJNR*.
- [24] M. Peres, O. Fedeli, B. Barrere, et al. "In Vivo Identification and monitoring of Changes in Rat Brain Glucose by Two-dimensional Shift-correlated  $^1\text{H}$  NMR Spectroscopy. *Magn Reson Med*, 1992.
- [25] J.K.M. Sanders, B.K. Hunter. *Modern NMR Spectroscopy: A Guide for Chemists*. Oxford, UK: Oxford University Press, 1987.
- [26] D. Shaw. "The Fundamental Principles of Nuclear Magnetic Resonance." *Biomedical Magnetic Resonance Imaging*, VCH Publishers, 1998: 1-46.
- [27] M. Sivaraja, C. Turner, K. Souza, S. Singer. "Ex Vivo Two-dimensional Proton Nuclear Magnetic Resonance Spectroscopy of Smooth Muscle Tumors: Advantages of Total Correlated Spectroscopy over Homonuclear J-correlated Spectroscopy." *Cancer Res*, 1994.
- [28] E.L. So. "Classification and Epidemiologic Considerations of Epileptic Seizures and Epilepsy." *Epilepsy*, 1995.
- [29] C.H. Sotak. "A Volume-localized, Two-dimensional NMR Method for the Determination of Lactate Using Zero-quantum Coherence Created in a Stimulated Echo Pulse Sequence." *Magn Reson Med*, 1988.
- [30] C.H. Sotak, D.M. Freeman, R.E. Hurd. "The Unequivocal determination of in vivo lactic acid using two-dimensional double quantum coherence transfer spectroscopy." *J. Magn Reson*, 1988.
- [31] Jonathan Sunshine, William C. Chan, Pamela J. Kassing. "Radiology Practices and Their Contracts with Hospitals, 1989-1990: A Representative Sample Survey." *American Journal of Roentgenology*, 1991.

- [32] M.A. Thomas, L.N. Ryner, M.P. Mehta, et al. "Localized 2D J-resolved  $^1\text{H}$  MR Spectroscopy of Human Brain Tumors In Vivo." *J Magn Reson Imaging*, 1996.
- [33] P.G. Williams, M.A. Helmer, L.C. Wright, et al. "Lipid Domain in Cancer Cell Plasma Membrane Shown in  $^1\text{H}$  NMR to be Similar to a Lipoprotein." *FEBS Lett* 1985.

## **Vita**

Carl Allen Fink was born in New Orleans, Louisiana, on 8 February 1981. He studied Computer Science at Loyola University New Orleans, where he received his Bachelor of Science in May 2003. Later that year, he moved to Baton Rouge and entered The Graduate School at Louisiana State University. He has held application development jobs at Entergy and the United States Naval Research Laboratory.